Optimal control of quantum systems: a projection approach

2005 J. Phys. A: Math. Gen. 38 929

(http://iopscience.iop.org/0305-4470/38/4/012)

INSTITUTE OF PHYSICS PUBLISHING JOURNAL OF PHYSICS A: MATHEMATICAL AND GENERAL

J. Phys. A: Math. Gen. **38** (2005) 929–942 doi:10.1088/0305-4470/38/4/012

Optimal control of quantum systems: a projection approach

Chao-Jung Cheng, Chi-Chuan Hwang, Teh-Lu Liao and Gen-Liang Chou

Department of Engineering Science, National Cheng Kung University, Tainan, 701 Taiwan, Republic of China

E-mail: tlliao@mail.ncku.edu.tw

Received 4 June 2004, in final form 5 November 2004
Published 12 January 2005
Online at stacks.iop.org/JPhysA/38/929

Abstract

This paper considers the optimal control of quantum systems. The controlled quantum systems are described by the probability-density-matrix-based Liouville–von Neumann equation. Using projection operators, the states of the quantum system are decomposed into two sub-spaces, namely the 'main state' space and the 'remaining state' space. Since the control energy is limited, a solution for optimizing the external control force is proposed in which the main state is brought to the desired main state at a certain target time, while the population of the remaining state is simultaneously suppressed in order to diminish its effects on the final population of the main state. The optimization problem is formulated by maximizing a general cost functional of states and control force. An efficient algorithm is developed to solve the optimization problem. Finally, using the hydrogen fluoride (HF) molecular population transfer problem as an illustrative example, the effectiveness of the proposed scheme for a quantum system initially in a mixed state or in a pure state is investigated through numerical simulations.

PACS number: 03.65.Ta

1. Introduction

The development and application of quantum control systems has attracted considerable academic attention in recent years [1–3]. Utilizing the principles of optimal control theory, various approaches have been developed for determining the control forces (laser pulses) to drive the quantum systems described by the Schrödinger equation or the Liouville–von Neumann equation in an optimal fashion in order to achieve a certain expected performance [4–17]. The density matrix framework in Liouville space is an efficient representation for the study of mixed-state quantum systems. The theory of optimal control in the density-matrix

formulation and its application to the generalized Tannor-Rice pump-dump molecular control scheme have been derived by Yan *et al* [7, 16]. To reduce the computational effort and increase the convergence rate in the optimization procedure, a monotonically convergent algorithm was developed which achieved the greatest transition probability from an initial state to an objective state while minimizing the control force [11, 15]. Furthermore, an extended algorithm was developed to treat another class of objective functionals for multiple target operations [17]. Meanwhile, a linear time-invariant (LTI) system for modelling a quantum system within short-time approximations was also developed in which a classical and local optimal control technique based on the so-called Riccati equation approach was derived [18]. However, this treatment is not applicable to quantum systems within which the wave packets bifurcate since these conditions prompt the mapping correlation between the wave packets and the classical particle to break down.

In general, a surrogate system can be employed to represent the dynamics of a quantum system using a lesser number of states [19, 20]. The states of the surrogate system can be defined in terms of the states of the whole system. Specifically, the states which are strongly coupled dominate the main dynamics of the quantum system, while those which are weakly coupled can generally be ignored. Therefore, complex high- or infinite-dimensional quantum systems can be represented by simplified low-dimensional models. It is worth noting, however, that the populations of the remaining quantum states are few but nevertheless existent and affect the control performance in a practical application. Consequently, a more effective approach for modelling quantum systems is required.

The application of projection approaches to the study of non-equilibrium statistical mechanics, no matter whether in classical or quantum systems, has been widely developed [21–25]. This approach can be used to derive the master equations by using a reduced density operator to describe the dynamics of a reduced system. Therefore, this technique not only reduces the number of degrees of freedom, but also determines theoretically the relationships between the quantum states of the reduced systems and those of the expanded systems. Moreover, the influence of the weakly coupled states on the strongly coupled states can be readily diminished by a suitably designed control field.

Drawing on the results of previous research, the present study commences from the Liouville–von Neumann equation and investigates non-equilibrium mixed-state quantum systems by means of the projection approach. Two projection operators are adopted, i.e., P and Q [21, 22]. These operators are employed to decompose the total state space of the quantum system into two sub-spaces, i.e., the 'main state' space (by operator P) and the 'remaining state' space (by operator Q). Since the control energy is limited, a solution for optimizing the external control force is proposed in which the main state is brought to the highest population at a certain target time, while the population of the remaining state is simultaneously suppressed in order to diminish its effects on the final population of the main state. The optimization problem is formulated by maximizing a general cost functional. A global and efficient algorithm is developed for the optimization process by adopting and modifying the entangled feedback algorithm introduced by Rabitz *et al* and Schirmer *et al* [6, 11]. Finally, the proposed method is applied to an HF molecular system to investigate its feasibility as an optimal control technique for selective vibrational state excitation.

The remainder of this paper is organized as follows. Section 2 presents the system formulations, while section 3 introduces the optimal control design and derives the numerical algorithm for the solution of the optimization process. Section 4 provides an illustrative example of the optimal population transition control of an HF molecular system and discusses the associated numerical simulation results. Finally, section 5 presents some brief conclusions.

2. System formulation

2.1. Liouville equation

Consider a quantum system described by the probability density operator, $\hat{\rho}(t)$, which evolves with time according to the *quantum Liouville* or Liouville–von Neumann equation, i.e.,

$$\frac{\partial}{\partial t}\hat{\rho}(t) = \frac{-\mathrm{i}}{\hbar}[\hat{H}(t), \hat{\rho}(t)] \tag{1}$$

where $\hat{H}(t)$ is the total Hamiltonian of the system and the initial state is $\hat{\rho}(t_0) = \hat{\rho}_0$.

The relationship between the probability density operator in Hilbert space and in Liouville space is generally established through the tetradic matrix [2]. Hence, the Liouville equation can be expressed in a similar form to that of the Schrödinger equation, i.e.,

$$\mathrm{i}\hbar\frac{\partial}{\partial t}|\hat{\rho}(t)\rangle\!\rangle = \hat{\mathcal{L}}(t)|\hat{\rho}(t)\rangle\!\rangle. \tag{2}$$

The initial state of equation (2) is given by $|\hat{\rho}(t_0)\rangle\!\rangle = |\hat{\rho}_0\rangle\!\rangle$, and $\hat{\mathcal{L}}(t)$ is the Liouville super-operator, which can be represented as a tetradic matrix.

A Liouville ket, $|\hat{A}\rangle\!\rangle$, and a Liouville bra, $\langle\!\langle\hat{A}|$, can be defined for the bounded operator, $\hat{A}$, evolved in Liouville space. The expected value of an observable $\hat{A}$ is defined by the inner product of $|\hat{\rho}(t)\rangle\!\rangle$ and $\langle\!\langle\hat{A}|$ in Liouville space, i.e.,

$$\langle\hat{A}\rangle = \mathrm{Tr}(\hat{A}\hat{\rho}(t)) = \langle\!\langle\hat{A}|\hat{\rho}(t)\rangle\!\rangle. \tag{3}$$

Furthermore, the time evolution operator, $\hat{S}(t, t_0)$, is defined for an arbitrary state $|\hat{\rho}(t)\rangle\!\rangle$ such that

$$|\hat{\rho}(t)\rangle\!\rangle = \hat{S}(t, t_0)|\hat{\rho}(t_0)\rangle\!\rangle. \tag{4}$$

Substituting equation (4) into equation (2) yields

$$\mathrm{i}\hbar\frac{\partial}{\partial t}\hat{S}(t, t_0) = \hat{\mathcal{L}}(t)\hat{S}(t, t_0). \tag{5}$$

The operator $\hat{S}(t, t_0)$ can be formally obtained as

$$\hat{\mathcal{S}}(t, t_0) \equiv \mathcal{T}_+ \exp\left[\frac{-\mathrm{i}}{\hbar}\int_{t_0}^{t}\hat{\mathcal{L}}(\tau)\,\mathrm{d}\tau\right] \tag{6}$$

where $\mathcal{T}_+$ indicates an increasing time order from right to left [22, 24].

Similarly, the transpose conjugate of $\hat{S}(t, t_0)$ can be derived as

$$\hat{\mathcal{S}}(t, t_0)^\dagger \equiv \mathcal{T}_- \exp\left[\frac{\mathrm{i}}{\hbar}\int_{t_0}^{t}\hat{\mathcal{L}}(\tau)\,\mathrm{d}\tau\right] \tag{7}$$

where $\mathcal{T}_-$ indicates an increasing time order from left to right.

2.2. Projection approach

This section develops a projection method for decomposing the state space of system (2) into two sub-spaces, i.e., the 'main quantum states' space, also known as the 'relevant' system, and the 'remaining quantum states' space, or the 'irrelevant' system.

Let P be the projection operator onto the sub-space composed of the 'main quantum states', which are the principal focus of the present study. Furthermore, let Q be the projection operator onto the remaining states, which are irrelevant. The operators P and Q satisfy the following conditions:

$$P^\dagger = P, \qquad Q^\dagger = Q, \qquad P^2 = P, \qquad Q^2 = Q, \qquad P + Q = I \tag{8}$$

and

$$PQ = QP = 0. \tag{9}$$

Appling the projection operators P and Q to equation (5) yields

$$\mathrm{i}\hbar\frac{\partial}{\partial t}P\hat{S}(t,t_0) = P\hat{\mathcal{L}}(t)P\hat{S}(t,t_0) + P\hat{\mathcal{L}}(t)Q\hat{S}(t,t_0) \tag{10}$$

$$\mathrm{i}\hbar\frac{\partial}{\partial t}Q\hat{S}(t,t_0) = Q\hat{\mathcal{L}}(t)P\hat{S}(t,t_0) + Q\hat{\mathcal{L}}(t)Q\hat{S}(t,t_0). \tag{11}$$

Multiplying equations (10) and (11) by the initial state, $|\hat{\rho}(t_0)\rangle\!\rangle$, and applying equation (4) gives:

$$\frac{\partial}{\partial t}P|\hat{\rho}(t)\rangle\!\rangle = P\left(\frac{-\mathrm{i}}{\hbar}\hat{\mathcal{L}}(t)\right)P|\hat{\rho}(t)\rangle\!\rangle + P\left(\frac{-\mathrm{i}}{\hbar}\hat{\mathcal{L}}(t)\right)Q|\hat{\rho}(t)\rangle\!\rangle \tag{12}$$

$$\frac{\partial}{\partial t}Q|\hat{\rho}(t)\rangle\!\rangle = Q\left(\frac{-\mathrm{i}}{\hbar}\hat{\mathcal{L}}(t)\right)P|\hat{\rho}(t)\rangle\!\rangle + Q\left(\frac{-\mathrm{i}}{\hbar}\hat{\mathcal{L}}(t)\right)Q|\hat{\rho}(t)\rangle\!\rangle. \tag{13}$$

The 'main quantum states' can be defined as $|\bar{\rho}(t)\rangle\!\rangle$ by $|\bar{\rho}(t)\rangle\!\rangle = P|\hat{\rho}(t)\rangle\!\rangle$, while the 'remaining quantum states' can be expressed as $|\rho'(t)\rangle\!\rangle$ by $|\rho'(t)\rangle\!\rangle = Q|\hat{\rho}(t)\rangle\!\rangle$. Utilizing the completeness property of the projection operators P and Q, it can be shown that an arbitrary mixed state of the quantum system is given by

$$|\hat{\rho}(t)\rangle\!\rangle = (P+Q)|\hat{\rho}(t)\rangle\!\rangle = |\bar{\rho}(t)\rangle\!\rangle + |\rho'(t)\rangle\!\rangle. \tag{14}$$

Furthermore equations (12) and (13) can be rewritten as

$$\frac{\partial}{\partial t}|\bar{\rho}(t)\rangle\!\rangle = P\left(\frac{-\mathrm{i}}{\hbar}\hat{\mathcal{L}}(t)\right)|\bar{\rho}(t)\rangle\!\rangle + P\left(\frac{-\mathrm{i}}{\hbar}\hat{\mathcal{L}}(t)\right)|\rho'(t)\rangle\!\rangle \tag{15}$$

$$\frac{\partial}{\partial t}|\rho'(t)\rangle\!\rangle = Q\left(\frac{-\mathrm{i}}{\hbar}\hat{\mathcal{L}}(t)\right)|\bar{\rho}(t)\rangle\!\rangle + Q\left(\frac{-\mathrm{i}}{\hbar}\hat{\mathcal{L}}(t)\right)|\rho'(t)\rangle\!\rangle. \tag{16}$$

These equations can also be expressed in the following compact form

$$\frac{\partial}{\partial t}|\boldsymbol{\rho}(t)\rangle\!\rangle \equiv \frac{\partial}{\partial t}\begin{bmatrix}|\bar{\rho}(t)\rangle\!\rangle\\ |\rho'(t)\rangle\!\rangle\end{bmatrix} = \frac{-\mathrm{i}}{\hbar}\begin{bmatrix}P\hat{\mathcal{L}} & P\hat{\mathcal{L}}\\ Q\hat{\mathcal{L}} & Q\hat{\mathcal{L}}\end{bmatrix}\begin{bmatrix}|\bar{\rho}(t)\rangle\!\rangle\\ |\rho'(t)\rangle\!\rangle\end{bmatrix} \equiv \frac{-\mathrm{i}}{\hbar}\mathbf{L}(t)|\boldsymbol{\rho}(t)\rangle\!\rangle. \tag{17}$$

Equation (17) governs the dynamics of the 'main quantum states', $|\bar{\rho}(t)\rangle\!\rangle$, and the 'remaining quantum states', $|\rho'(t)\rangle\!\rangle$. Hence, this equation is the key equation for the optimal control force design.

3. Optimal control design

3.1. Optimal control problem

Consider a quantum system represented by equation (1) with M external control linear forces. The total Hamiltonian of this system can be expressed by

$$\hat{H}(t) = \hat{H}_0 + \sum_{m=1}^{M} u_m(t)\hat{H}_m \tag{18}$$

where $\hat{H}_0$ is the Hamiltonian of the unperturbed system and $\hat{H}_m$ is the corresponding interaction Hamiltonian with the control field, $u_m(t)$.

In this case, the corresponding Liouville super-operator is given by

$$\hat{\mathcal{L}}(t) = \hat{\mathcal{L}}_0 + \sum_{m=1}^{M} u_m(t)\hat{\mathcal{L}}_m. \tag{19}$$

When the bounded and real-valued external control field is defined in the time interval $[t_0, t_F]$ and the initial state $|\hat{\rho}_0\rangle\!\rangle$ is given, then the time evolution of the system states can be solved by equation (2) or by equations (4) and (6). However, with the projection operators P and Q, the main state, $|\bar{\rho}(t)\rangle\!\rangle$, and the remaining state, $|\rho'(t)\rangle\!\rangle$, can be determined by solving equations (15) and (16).

This paper now considers the control problem associated with determining the bounded external forces $u_m(t)$, $m = 1, \ldots, M$ within the time interval $[t_0, t_F]$, such that equation (2) is satisfied subject to the following constraints, which are consolidated in the so-called *optimal criteria*: (i) the control forces bring the main state to the desired target at a time t_F; (ii) the control strengths are minimized as a result of the limited control energy; (iii) the populations of the remaining states $|\rho'(t_F)\rangle\!\rangle$ at time t_F are suppressed in order to diminish its effects on the final population of the main state. These constraints can be summarized in the form of a cost functional, i.e.,

$$J(\bar{\rho}, \rho', u_1, \ldots, u_M) = \langle\!\langle \hat{A}|\bar{\rho}(t_F)\rangle\!\rangle - \langle\!\langle \hat{A}'|\rho'(t_F)\rangle\!\rangle - \sum_{m=1}^{M} \frac{w_m}{2\hbar} \int_{t_0}^{t_F} [u_m(t)]^2 \, \mathrm{d}t \tag{20}$$

where w_m are weighting parameters, which indicate the relative concerns of the control forces, $\hat{A}$ are the observable quantities which are to be controlled and $\hat{A}'$ are the suppressed quantities.

For example, in the control of population transfers, a certain energy level $|n\rangle$ represents the target state, i.e. $\hat{A}$, while the other states $|l\rangle$, $l \neq n$, i.e. $\hat{A}'$, are to be restrained. Hence, the choice of $\hat{A}'$ relies on the specific control goals. The optimal control can then be rewritten as

$$\max J(\bar{\rho}, \rho', u_1, \ldots, u_M) \text{ subject to (15) and (16).} \tag{21a}$$

The constrained optimization problem of equation (21*a*) can be transformed into an unconstrained case via the use of Lagrange multipliers. The Lagrangian function can be expressed as follows:

$$\begin{aligned} L(\bar{\rho}, \rho', u_1, \ldots, u_M, \lambda_1, \lambda_2) &= J(\bar{\rho}, \rho', u_1, \ldots, u_M) \\ &+ \int_{t_0}^{t_F} \langle\!\langle \boldsymbol{\lambda}_1(t)|\mathbf{F}_1(t)\rangle\!\rangle \, \mathrm{d}t + \int_{t_0}^{t_F} \langle\!\langle \boldsymbol{\lambda}_2(t)|\mathbf{F}_2(t)\rangle\!\rangle \, \mathrm{d}t \end{aligned} \tag{21b}$$

and

$$\mathbf{F}_1(t) = \frac{\partial}{\partial t}|\bar{\rho}(t)\rangle\!\rangle + \frac{\mathrm{i}}{\hbar} P\hat{\mathcal{L}}(t)[|\bar{\rho}(t)\rangle\!\rangle + |\rho'(t)\rangle\!\rangle] = \mathbf{0}$$

$$\mathbf{F}_2(t) = \frac{\partial}{\partial t}|\rho'(t)\rangle\!\rangle + \frac{\mathrm{i}}{\hbar} Q\hat{\mathcal{L}}(t)[|\bar{\rho}(t)\rangle\!\rangle + |\rho'(t)\rangle\!\rangle] = \mathbf{0}$$

where $|\boldsymbol{\lambda}_1(t)\rangle\!\rangle$ and $|\boldsymbol{\lambda}_2(t)\rangle\!\rangle$ are quantum Lagrange multipliers.

To determine the necessary conditions which maximize the solution of equation (21*b*), the calculus of variations for equation (21*b*) are taken with the initial conditions of states $|\bar{\rho}(t_0)\rangle\!\rangle = |\bar{\rho}_0\rangle\!\rangle$ and $|\rho'(t_0)\rangle\!\rangle = |\rho'_0\rangle\!\rangle$.

$$\begin{aligned} \delta L \equiv \frac{\partial L}{\partial|\lambda_1(t)\rangle\!\rangle}\delta|\lambda_1(t)\rangle\!\rangle + \frac{\partial L}{\partial|\lambda_2(t)\rangle\!\rangle}\delta|\lambda_2(t)\rangle\!\rangle + \frac{\partial L}{\partial|\bar{\rho}(t_F)\rangle\!\rangle}\bigg|_{t_F}\delta|\bar{\rho}(t_F)\rangle\!\rangle \\ + \frac{\partial L}{\partial|\rho'(t_F)\rangle\!\rangle}\bigg|_{t_F}\delta|\rho'(t_F)\rangle\!\rangle + \frac{\partial L}{\partial|\bar{\rho}(t)\rangle\!\rangle}\delta|\bar{\rho}(t)\rangle\!\rangle + \frac{\partial L}{\partial|\rho'(t)\rangle\!\rangle}\delta|\rho'(t)\rangle\!\rangle + \frac{\partial L}{\partial u}\delta u. \end{aligned} \tag{22}$$

Hence, the Euler–Lagrange equations can be obtained as

$$\begin{cases} \dfrac{\partial}{\partial t}|\bar{\rho}(t)\rangle\!\rangle + \dfrac{\mathrm{i}}{\hbar} P\hat{\mathcal{L}}(t)[|\bar{\rho}(t)\rangle\!\rangle + |\rho'(t)\rangle\!\rangle] = \mathbf{0} \\ \dfrac{\partial}{\partial t}|\rho'(t)\rangle\!\rangle + \dfrac{\mathrm{i}}{\hbar} Q\hat{\mathcal{L}}(t)[|\bar{\rho}(t)\rangle\!\rangle + |\rho'(t)\rangle\!\rangle] = \mathbf{0} \end{cases} \tag{23}$$

with $|\bar{\rho}(t_0)\rangle\!\rangle = |\bar{\rho}_0\rangle\!\rangle$, $|\rho'(t_0)\rangle\!\rangle = |\rho'_0\rangle\!\rangle$

$$\begin{bmatrix} |\dot{\boldsymbol{\lambda}}_1(t)\rangle\!\rangle \\ |\dot{\boldsymbol{\lambda}}_2(t)\rangle\!\rangle \end{bmatrix} + \frac{\mathrm{i}}{\hbar} \begin{bmatrix} \hat{\mathcal{L}}(t)P & \hat{\mathcal{L}}(t)Q \\ \hat{\mathcal{L}}(t)P & \hat{\mathcal{L}}(t)Q \end{bmatrix} \begin{bmatrix} |\boldsymbol{\lambda}_1(t)\rangle\!\rangle \\ |\boldsymbol{\lambda}_2(t)\rangle\!\rangle \end{bmatrix} = \begin{bmatrix} \mathbf{0} \\ \mathbf{0} \end{bmatrix} \tag{24}$$

with

$$\begin{bmatrix} |\boldsymbol{\lambda}_1(t_F)\rangle\!\rangle \\ |\boldsymbol{\lambda}_2(t_F)\rangle\!\rangle \end{bmatrix} = \begin{bmatrix} |\hat{A}\rangle\!\rangle \\ -|\hat{A}'\rangle\!\rangle \end{bmatrix} \tag{25}$$

$$u_m(t) = \mathrm{Re}\left(\frac{-\mathrm{i}\langle\!\langle \boldsymbol{\lambda}_1(t)|P\hat{\mathcal{L}}_m|\bar{\rho}(t) + \rho'(t)\rangle\!\rangle}{w_m} - \frac{\mathrm{i}\langle\!\langle \boldsymbol{\lambda}_2(t)|Q\hat{\mathcal{L}}_m|\bar{\rho}(t) + \rho'(t)\rangle\!\rangle}{w_m} \right)$$
$$m = 1, 2, \ldots, M. \tag{26}$$

Note that the state equation (equation (23)) evolves forward in time, while the adjoint equation (equation (24)) evolves backwards. Equation (26) provides the control forces.

3.2. Numerical algorithm

This study adopts and modifies the entangled feedback algorithm developed by Rabitz *et al* and Schirmer *et al* [6, 11] to solve the coupled equations (equations (23)–(26)). The procedures of the numerical algorithm can be summarized as follows:

Step 0. Let the time interval $[t_0, t_F]$ be divided into F tiny sub-intervals of equal step size, $\Delta t = t_{n+1} - t_n = \frac{t_F - t_0}{F}$.

Step 1. Guess the initial control fields $u_m(t) = u_m^0(t)$, $m = 1, 2, \ldots, M$, and substitute these fields into equations (15) and (16), i.e.,

$$\frac{\partial}{\partial t}|\bar{\rho}(t)\rangle\!\rangle = -\frac{\mathrm{i}}{\hbar} P\left(\hat{\mathcal{L}}_0 + \sum_{m=1}^{M} u_m^0(t)\hat{\mathcal{L}}_m\right)[|\bar{\rho}(t)\rangle\!\rangle + |\rho'(t)\rangle\!\rangle] \tag{27a}$$

$$\frac{\partial}{\partial t}|\rho'(t)\rangle\!\rangle = -\frac{\mathrm{i}}{\hbar} Q\left(\hat{\mathcal{L}}_0 + \sum_{m=1}^{M} u_m^0(t)\hat{\mathcal{L}}_m\right)[|\bar{\rho}(t)\rangle\!\rangle + |\rho'(t)\rangle\!\rangle] \tag{27b}$$

with $|\bar{\rho}(t_0)\rangle\!\rangle = |\bar{\rho}_0\rangle\!\rangle$ and $|\rho'(t_0)\rangle\!\rangle = |\rho'_0\rangle\!\rangle$.

The density evolutions $|\bar{\rho}^0(t)\rangle\!\rangle$ and $|\rho'^0(t)\rangle\!\rangle$ are solved by means of a symmetric split operator method as shown below in *Step* 4 with a step size of Δt.

Step 2. For the jth iteration ($j \geqslant 1$) and $k = 0, 1$, define

$$\hat{\mathcal{L}}^{j,k}(t) \equiv \hat{\mathcal{L}}_0 + \sum_{m=1}^{M} u_m^{j,k}(t)\hat{\mathcal{L}}_m, \tag{28}$$

where

$$u_m^{j,k}(t) = \mathrm{Re}\left\{ -\frac{\mathrm{i}\langle\!\langle \boldsymbol{\lambda}_1^j(t)\big|P\hat{\mathcal{L}}_m\big|\bar{\rho}^{j-k}(t) + \rho'^{j-k}(t)\rangle\!\rangle + \mathrm{i}\langle\!\langle \boldsymbol{\lambda}_2^j(t)\big|Q\hat{\mathcal{L}}_m\big|\bar{\rho}^{j-k}(t) + \rho'^{j-k}(t)\rangle\!\rangle}{w_m} \right\} \tag{29}$$

is derived from equation (26). The Lagrange multipliers ($k = 1$) and density operators ($k = 0$) are then determined iteratively by the following equations deduced from equations (23) and (24):

$$\frac{\partial}{\partial t}\left|\lambda_1^j(t)\right\rangle\!\!\right\rangle = -\frac{\mathrm{i}}{\hbar}\left(\hat{\mathcal{L}}^{j,1}(t)P\left|\lambda_1^j(t)\right\rangle\!\!\right\rangle + \hat{\mathcal{L}}^{j,1}(t)Q\left|\lambda_2^j(t)\right\rangle\!\!\right\rangle\right) \tag{30a}$$

$$\frac{\partial}{\partial t}\left|\lambda_2^j(t)\right\rangle\!\!\right\rangle = -\frac{\mathrm{i}}{\hbar}\left(\hat{\mathcal{L}}^{j,1}(t)P\left|\lambda_1^j(t)\right\rangle\!\!\right\rangle + \hat{\mathcal{L}}^{j,1}(t)Q\left|\lambda_2^j(t)\right\rangle\!\!\right\rangle\right) \tag{30b}$$

with $\left|\lambda_1^j(t_F)\right\rangle\!\!\right\rangle = |\hat{A}\rangle\!\rangle$ and $\left|\lambda_2^j(t_F)\right\rangle\!\!\right\rangle = -|\hat{A}'\rangle\!\rangle$

$$\frac{\partial}{\partial t}|\bar{\rho}^j(t)\rangle\!\rangle = -\frac{\mathrm{i}}{\hbar}P\hat{\mathcal{L}}^{j,0}(t)[|\bar{\rho}^j(t)\rangle\!\rangle + |\rho'^j(t)\rangle\!\rangle] \tag{31a}$$

$$\frac{\partial}{\partial t}|\rho'^j(t)\rangle\!\rangle = -\frac{\mathrm{i}}{\hbar}Q\hat{\mathcal{L}}^{j,0}(t)[|\bar{\rho}^j(t)\rangle\!\rangle + |\rho'^j(t)\rangle\!\rangle] \tag{31b}$$

with $|\bar{\rho}^j(t_0)\rangle\!\rangle = |\bar{\rho}_0\rangle\!\rangle$ and $|\rho'^j(t_0)\rangle\!\rangle = |\rho_0'\rangle\!\rangle$.

Step 3. The control fields of the jth iteration are calculated from equation (29) for $k = 0$:

$$u_m^j(t) \equiv u_m^{j,0}(t) = \mathrm{Re}\left\{\frac{-\mathrm{i}\left\langle\!\left\langle\lambda_1^j(t)|P\hat{\mathcal{L}}_m|\bar{\rho}^j(t) + \rho'^j(t)\right\rangle\!\right\rangle}{w_m} - \frac{\mathrm{i}\left\langle\!\left\langle\lambda_2^j(t)|Q\hat{\mathcal{L}}_m|\bar{\rho}^j(t) + \rho'^j(t)\right\rangle\!\right\rangle}{w_m}\right\}. \tag{32}$$

Step 4. Calculate the variation of the cost functional for two successive iterations $\delta J^{j,j-1}$ by

$$\delta J^{j,j-1} = \langle\!\langle\hat{A}|\bar{\rho}^j(t_F)\rangle\!\rangle - \langle\!\langle\hat{A}|\bar{\rho}^{j-1}(t_F)\rangle\!\rangle - \langle\!\langle\hat{A}'|\rho'^j(t_F)\rangle\!\rangle + \langle\!\langle\hat{A}'|\rho'^{j-1}(t_F)\rangle\!\rangle + \sum_{m=1}^{M}\frac{w_m}{2\hbar}\int_{t_0}^{t_F}\left[u_m^{j-1}(t)\right]^2 - \left[u_m^j(t)\right]^2\mathrm{d}t. \tag{33}$$

A symmetric split operator method is applied to solve $|\bar{\rho}^j(t)\rangle\!\rangle$ and $|\rho'^j(t)\rangle\!\rangle$, respectively, i.e.,

(a) Using $\hat{\mathrm{S}}(t, t_0)$ of equation (6) and marching forward gives

$$\begin{aligned}\begin{bmatrix}|\bar{\rho}^j(t_{n+1})\rangle\!\rangle\\ |\rho'^j(t_{n+1})\rangle\!\rangle\end{bmatrix} \approx{}& \exp\left(-\frac{\mathrm{i}\Delta t}{2\hbar}\mathbf{L}_0\right)\exp\left(-\frac{\mathrm{i}\Delta t}{2\hbar}u_1^{j,0}(\tau_n)\mathbf{L}_1\right)\cdots\exp\left(-\frac{\mathrm{i}\Delta t}{2\hbar}u_M^{j,0}(\tau_n)\mathbf{L}_M\right)\\ &\times\exp\left(-\frac{\mathrm{i}\Delta t}{2\hbar}u_M^{j,0}(\tau_n)\mathbf{L}_M\right)\cdots\exp\left(-\frac{\mathrm{i}\Delta t}{2\hbar}u_1^{j,0}(\tau_n)\mathbf{L}_1\right)\exp\left(-\frac{\mathrm{i}\Delta t}{2\hbar}\mathbf{L}_0\right)\\ &\times\begin{bmatrix}|\bar{\rho}^j(t_n)\rangle\!\rangle\\ |\rho'^j(t_n)\rangle\!\rangle\end{bmatrix}\qquad n = 0, 1, \ldots, F-1\end{aligned} \tag{34}$$

where

$$\mathbf{L}_m = \begin{bmatrix}P\hat{\mathcal{L}}_m & P\hat{\mathcal{L}}_m\\ Q\hat{\mathcal{L}}_m & Q\hat{\mathcal{L}}_m\end{bmatrix}\qquad m = 0, 1, \ldots, M.$$

(b) Using $\hat{\mathrm{S}}(t, t_0)^\dagger$ of equation (7) and marching backward gives

$$\begin{aligned}\begin{bmatrix}|\lambda_1^j(t_n)\rangle\!\rangle\\ |\lambda_2^j(t_n)\rangle\!\rangle\end{bmatrix} \approx{}& \exp\left(\frac{\mathrm{i}\Delta t}{2\hbar}\mathbf{L}_0^\dagger\right)\exp\left(\frac{\mathrm{i}\Delta t}{2\hbar}u_1^{j,1}(\tau_n)\mathbf{L}_1^\dagger\right)\cdots\exp\left(\frac{\mathrm{i}\Delta t}{2\hbar}u_M^{j,1}(\tau_n)\mathbf{L}_M^\dagger\right)\\ &\times\exp\left(\frac{\mathrm{i}\Delta t}{2\hbar}u_M^{j,1}(\tau_n)\mathbf{L}_M^\dagger\right)\cdots\exp\left(\frac{\mathrm{i}\Delta t}{2\hbar}u_1^{j,1}(\tau_n)\mathbf{L}_1^\dagger\right)\\ &\times\exp\left(\frac{\mathrm{i}\Delta t}{2\hbar}\mathbf{L}_0^\dagger\right)\begin{bmatrix}|\lambda_1^j(t_{n+1})\rangle\!\rangle\\ |\lambda_2^j(t_{n+1})\rangle\!\rangle\end{bmatrix}\qquad n = F-1, F-2, \ldots, 0\end{aligned} \tag{35}$$

where

$$\begin{cases} \tau_n = t_n + \dfrac{\Delta t}{2} = t_{n+1} - \dfrac{\Delta t}{2} \\ u_m^{j,k}\left(t_n \pm \dfrac{\Delta t}{2}\right) \approx u_m^{j,k}(t_n) \pm \left.\dfrac{du_m^{j,k}(t)}{dt}\right|_{t_n} \times \dfrac{\Delta t}{2} \end{cases}$$

and

$$u_m^{j,k}\left(t_n \pm \frac{\Delta t}{2}\right) \approx u_m^{j,k}(t_n) \pm \frac{1}{\hbar w_m}\left\{\left\langle\left\langle \boldsymbol{\lambda}_1^j(t_n)\right| P[\hat{\mathcal{L}}_0, \hat{\mathcal{L}}_m]\left|(\bar{\rho}^{j-k}(t_n) + \rho'^{j-k}(t_n))\right\rangle\right\rangle + \left\langle\left\langle \boldsymbol{\lambda}_2^j(t_n)\right| \{Q[\hat{\mathcal{L}}_0, \hat{\mathcal{L}}_m]\left|(\bar{\rho}^{j-k}(t_n) + \rho'^{j-k}(t_n))\right\rangle\right\rangle\right\} \times \frac{\Delta t}{2} \quad (m = 1, 2, \ldots, M). \tag{36}$$

Step 5. If $\delta J^{j,j-1} \leqslant \varepsilon$ and $j \geqslant 150$, where ε is a pre-specified positive and small constant, then the iteration is terminated; otherwise the procedure returns to step 2.

4. An illustrative example

To investigate the performance of the proposed projection approach, this study investigates the optimization control problem for a system of diatomic HF molecules described by the Morse oscillator potential model or harmonic oscillator model with N vibrational states $|n\rangle$ corresponding to energy levels E_n [3, 8, 11].

The unperturbed part of the Hamiltonian operator is given by

$$\hat{H}_0 = \sum_{n=1}^{N} E_n |n\rangle\langle n| \tag{37}$$

where

$$E_n = \hbar\omega_0\left(n - \frac{1}{2}\right)\left[1 - \frac{1}{2}\left(n - \frac{1}{2}\right)B\right] \qquad n = 1, 2, \ldots < \frac{1}{B} + \frac{1}{2} \tag{38a}$$

$$\hbar\omega_0 = 2BD, \qquad B = \frac{\hbar a}{\sqrt{2\mu D}} \tag{38b}$$

where $B = 0.0419$, $D = 6.125\,\text{eV}$, $\omega_0/2\pi = 7.8\times10^{14}\,\text{s}^{-1}$, $\mu = 0.95\,\text{amu}$ and $d_n = 0.097\sqrt{n}$ Debye. Assume the diatomic molecular system is controlled by a single laser field, $u(t)$. Hence, the total Hamiltonian can be approximated by

$$\hat{H}(t) = \hat{H}_0 + u(t)\hat{H}_1 \tag{39a}$$

where $\hat{H}_1 = \sum_{n=1}^{N-1} d_n(|n\rangle\langle n+1| + |n+1\rangle\langle n|)$ is chosen to be of the dipole form and d_n denotes the transition dipole moments.

The corresponding Liouville super-operator is given by

$$\hat{\mathcal{L}}(t) = \hat{\mathcal{L}}_0 + u_1(t)\hat{\mathcal{L}}_1. \tag{39b}$$

From equation (38*a*), it can be shown that the system has 24 vibrational states. To simplify the analysis, the present study takes an HF molecule with four levels as a simplified model. The initial density operator is given by a mixed state:

$$\hat{\rho}(t_0) = \begin{bmatrix} 0.3850 & 0 & 0 & 0 \\ 0 & 0.2758 & 0 & 0 \\ 0 & 0 & 0.1976 & 0 \\ 0 & 0 & 0 & 0.1416 \end{bmatrix}. \tag{40}$$

The criterion of controllability [12] pointed out this HF Morse oscillator model is completely controllable. The control objective is to maximize the energy of the system; that is, to design the external control field such that the population of the most energetic state $|n = 4\rangle$ at target time $t_F = 200$ (au) is maximized, the second most energetic state $|n = 3\rangle$ has the second highest population, etc [8, 11].

According to the control objective and the kinematical bounds $\langle \hat{H}_0(t_f)\rangle \leqslant 2.2592\hbar\omega_0$ predicted theoretically in [8], the observable in the main state is specified as follows:

$$\hat{A} = \begin{bmatrix} 0 & 0 & 0 & 0 \\ 0 & E_2 & 0 & 0 \\ 0 & 0 & E_3 & 0 \\ 0 & 0 & 0 & E_4 \end{bmatrix} = \begin{bmatrix} 0 & 0 & 0 & 0 \\ 0 & 1.452\,86 & 0 & 0 \\ 0 & 0 & 2.369\,06 & 0 \\ 0 & 0 & 0 & 3.2434 \end{bmatrix} \tag{41}$$

Meanwhile, let $\hat{A}'$ in equation (20) and (33) satisfy

$$\hat{A}' = \hat{A}'_1 = \begin{bmatrix} E_1 & 0 & 0 & 0 \\ 0 & 0 & 0 & 0 \\ 0 & 0 & 0 & 0 \\ 0 & 0 & 0 & 0 \end{bmatrix} = \begin{bmatrix} 0.494\,76 & 0 & 0 & 0 \\ 0 & 0 & 0 & 0 \\ 0 & 0 & 0 & 0 \\ 0 & 0 & 0 & 0 \end{bmatrix}. \tag{42}$$

The proposed projection approach is applied by using the following operators:

$$P = \begin{bmatrix} 0 & 0 & 0 & 0 \\ 0 & 1 & 0 & 0 \\ 0 & 0 & 1 & 0 \\ 0 & 0 & 0 & 1 \end{bmatrix}, \qquad Q = \begin{bmatrix} 1 & 0 & 0 & 0 \\ 0 & 0 & 0 & 0 \\ 0 & 0 & 0 & 0 \\ 0 & 0 & 0 & 0 \end{bmatrix} \tag{43}$$

with the conditions given in equations (40)–(42) and $w_m = 8$. In this mixed-state case, states $|2\rangle$, $|3\rangle$ and $|4\rangle$ are regarded as the main quantum states generated through the operation of P. Moreover, in this case, we assumed the state $|1\rangle$ as a remaining state generated through the operation of Q, and want to diminish its effect on the final population of the main states $|2\rangle$, $|3\rangle$ and $|4\rangle$.

Figure 1 shows the control field with the conditions of equations (40)–(43). Meanwhile, figure 2 depicts the corresponding time-evolution populations of each energy level of the $N = 4$ quantum system when applying the proposed projection approach. The populations of states $|1\rangle$, $|2\rangle$, $|3\rangle$ and $|4\rangle$ at the target time are 0.1490, 0.1993, 0.2756 and 0.3763, respectively. The final energy is $2.2367\hbar\omega_0$ or about 99.01% of the kinematical upper bound. We carry out similar simulations for a four-level Morse oscillator model initially in ground state:

$$\hat{\rho}(t_0) = \begin{bmatrix} 1 & 0 & 0 & 0 \\ 0 & 0 & 0 & 0 \\ 0 & 0 & 0 & 0 \\ 0 & 0 & 0 & 0 \end{bmatrix}. \tag{44}$$

In this pure state case, to maximize the energy of the system is to attain a nearly complete inversion of the populations so that the population of state $|4\rangle$ is close to 1. Thus, the observable can be the population of state $|4\rangle$ and specified as follows:

$$\hat{A} = \begin{bmatrix} 0 & 0 & 0 & 0 \\ 0 & 0 & 0 & 0 \\ 0 & 0 & 0 & 0 \\ 0 & 0 & 0 & 1 \end{bmatrix} \tag{45}$$

and the following projection operators are chosen:

$$P = \begin{bmatrix} 0 & 0 & 0 & 0 \\ 0 & 0 & 0 & 0 \\ 0 & 0 & 0 & 0 \\ 0 & 0 & 0 & 1 \end{bmatrix}, \qquad Q = \begin{bmatrix} 1 & 0 & 0 & 0 \\ 0 & 1 & 0 & 0 \\ 0 & 0 & 1 & 0 \\ 0 & 0 & 0 & 0 \end{bmatrix}. \tag{46}$$

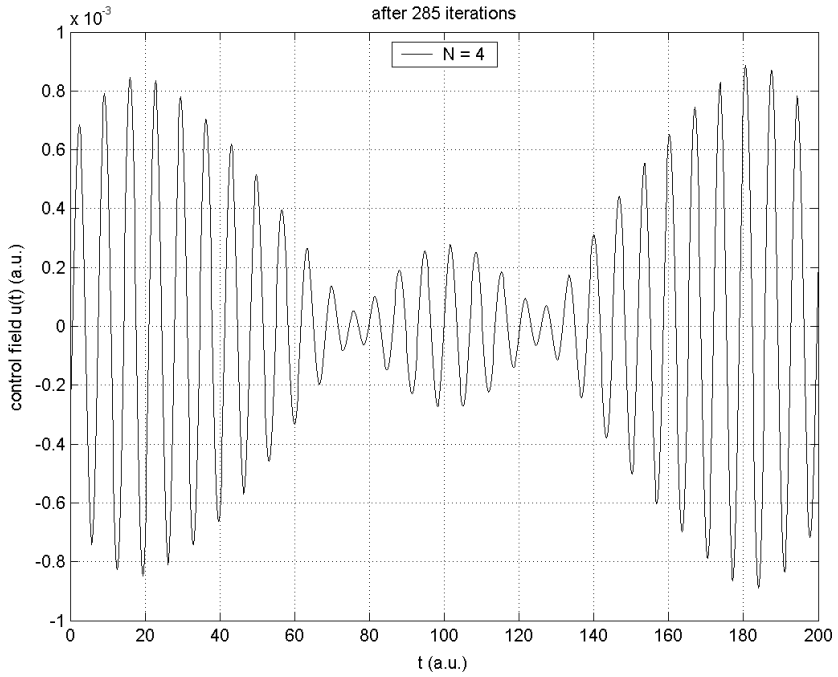

Figure 1. Optimized control field for a mixed-state quantum system with $w_m = 8$ ($N = 4$ Morse oscillator).

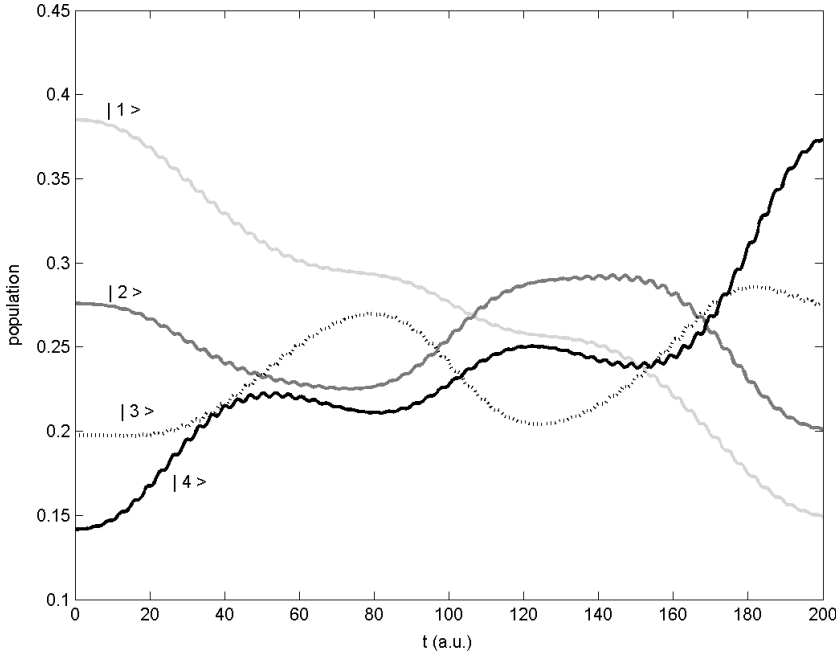

Figure 2. Time evolution of populations for a mixed-state quantum system ($N = 4$ Morse oscillator).

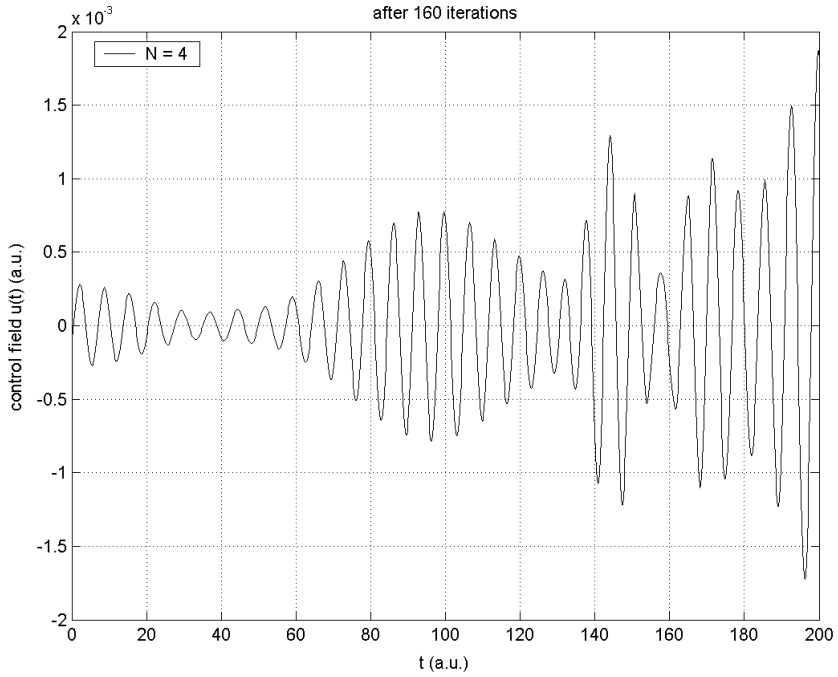

Figure 3. Optimized control field for a pure state quantum system with $w_m = 4$ ($N = 4$ Morse oscillator).

State $|4\rangle$ is regarded as the main quantum state generated through the operation of P. Furthermore, in this case, we considered the states $|1\rangle$, $|2\rangle$ and $|3\rangle$ as remaining states generated through the operation of Q. Figure 3 shows the control field with the conditions of equations (44)–(46) and $w_m = 4$. Figure 4 depicts the corresponding time-evolution populations of each energy level of the $N = 4$ quantum system. The population of state $|4\rangle$ at the target time is approximately close to 0.993. Compared with the above-mentioned completely controllable Morse oscillator model, we consider the HF molecular system as a four-level harmonic oscillator model with the same E_1 and E_2 as equation (38*a*) but E_3 and E_4 adjusted to achieve equal spacing of adjacent energy levels. This model is not completely controllable and its kinematical upper bound is predicted by $\langle \hat{H}_0(t_f)\rangle \leqslant 2.3192\hbar\omega_0$ [8]. We perform numerical simulation for the system with an initial mixed state as given in equation (40) and the observable $\hat{A}$ and $\hat{A}'$ are chosen as follows, respectively:

$$\hat{A} = \begin{bmatrix} 0 & 0 & 0 & 0 \\ 0 & 0 & 0 & 0 \\ 0 & 0 & 1 & 0 \\ 0 & 0 & 0 & 2.9693 \end{bmatrix}, \qquad \hat{A}' = \begin{bmatrix} 0.494\,76 & 0 & 0 & 0 \\ 0 & 1.452\,86 & 0 & 0 \\ 0 & 0 & 0 & 0 \\ 0 & 0 & 0 & 0 \end{bmatrix} \tag{47}$$

The projection operators are chosen as shown in equation (48).

$$P = \begin{bmatrix} 0 & 0 & 0 & 0 \\ 0 & 0 & 0 & 0 \\ 0 & 0 & 1 & 0 \\ 0 & 0 & 0 & 1 \end{bmatrix}, \qquad Q = \begin{bmatrix} 1 & 0 & 0 & 0 \\ 0 & 1 & 0 & 0 \\ 0 & 0 & 0 & 0 \\ 0 & 0 & 0 & 0 \end{bmatrix}. \tag{48}$$

Figure 5 shows the optimal control field with the conditions of equations (40) and (47). Figure 6 depicts the corresponding time-evolution populations of each energy level of the

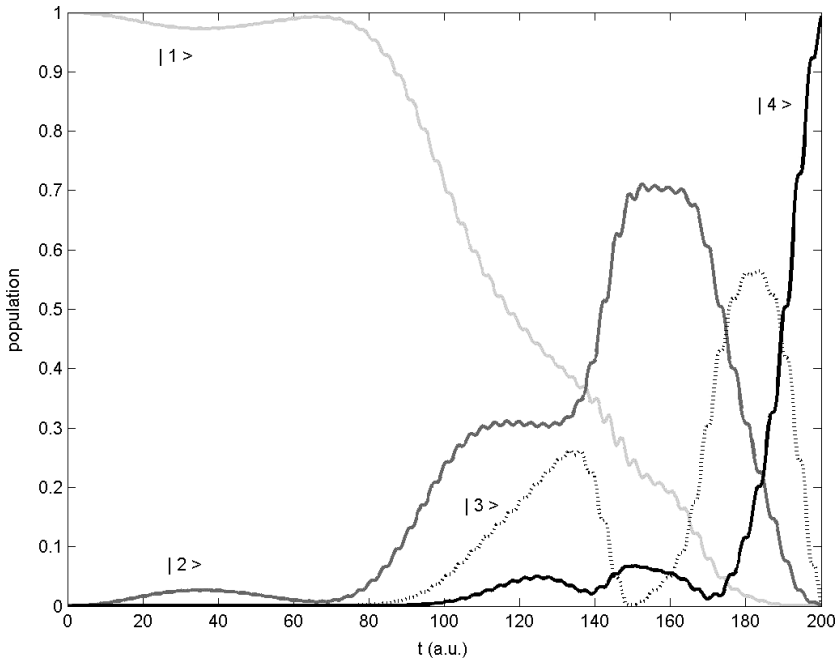

Figure 4. Time evolution of populations for a pure state quantum system ($N = 4$ Morse oscillator).

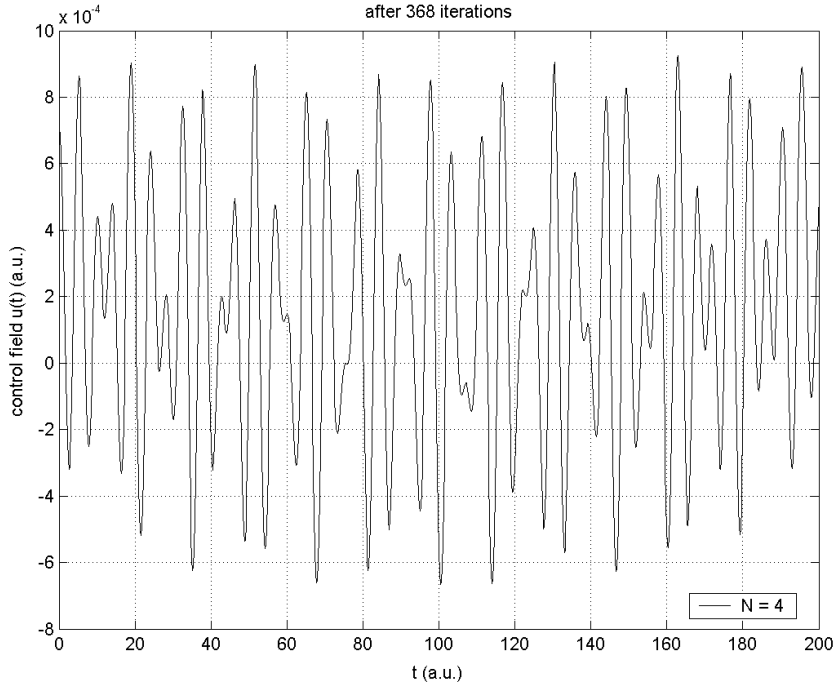

Figure 5. Optimized control field for a mixed-state quantum system with $w_m = 8$ ($N = 4$ harmonic oscillator).

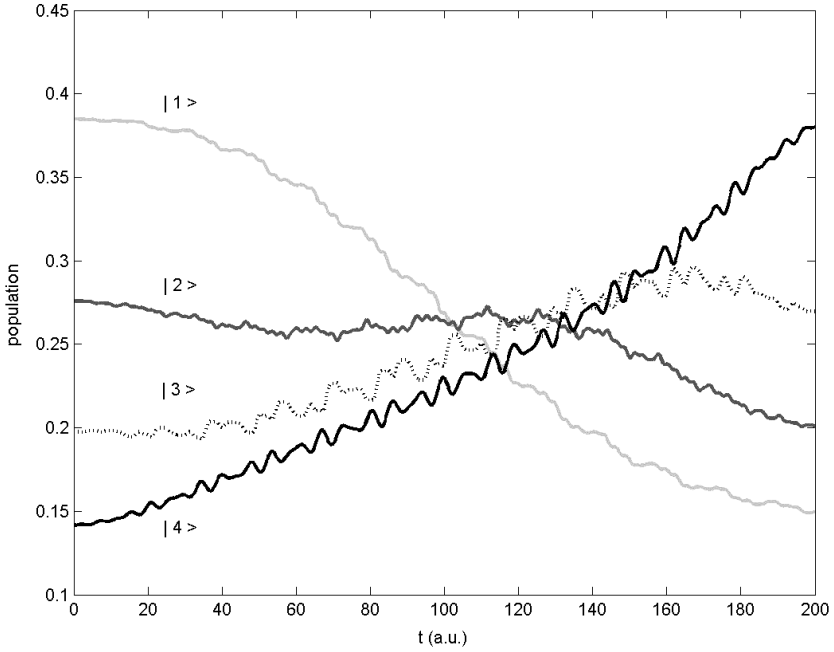

Figure 6. Time evolution of populations for a mixed-state quantum system ($N = 4$ harmonic oscillator).

$N = 4$ quantum system. The populations of states $|1\rangle$, $|2\rangle$, $|3\rangle$ and $|4\rangle$ at the target time are 0.1513, 0.1989, 0.2708 and 0.3789, respectively. The final energy is $2.295\hbar\omega_0$ or about 98.87% of the kinematical upper bound, which may be dynamically realizable for a particular choice of observable in this simulation. However, it is worth noting that kinematical attainability does not imply dynamically reachable [8].

5. Conclusions

This paper has developed an optimal control approach for quantum systems which evolve in Liouville space. Using projection operators, the states of the quantum system are decomposed into two sub-spaces, namely the 'main state' space and the 'remaining state' space. Since the control energy is limited, this study has proposed a solution for the optimization of the external control force in which the main state is brought to the highest population at a certain target time, t_F, while the population of the remaining state is simultaneously suppressed in order to diminish its effects on the final population of the main state. A numerical algorithm for the optimization solution has also been presented and indicates its applicable potential of the scheme by considering the energy maximization problem or state transition optimal control of an HF molecular quantum system initially in pure state or mixed-state condition. We believe that this proposed scheme in this study may provide as an alternative approach for the optimal control of quantum systems and its effectiveness has been shown as good as that proposed by [8, 11]. However, more efficient algorithms for the projection approach should be further studied.

Acknowledgment

This research was supported by the National Science Council, Republic of China, under Grant NSC 92-2218-E-006-107.

References

[1] Warren W S, Rabitz H and Dahleh M A 1993 *Science* **259** 1581
[2] Ohtsuki Y and Fujimura Y 1989 *J. Chem. Phys.* **91** 3903
[3] Chelkowski S, Bandrauk A D and Corkum P B 1990 *Phys. Rev. Lett.* **65** 2355
[4] Shi S, Woody A and Rabitz H 1988 *J. Chem. Phys.* **88** 6870
[5] Shi S and Rabitz H 1990 *J. Chem. Phys.* **92** 2927
[6] Zhu W and Rabitz H 1998 *J. Chem. Phys.* **109** 385
[7] Yan Y 1994 *J. Chem. Phys.* **100** 1094
[8] Girardeau M D, Schirmer S G, Leahy J V and Koch R M 1998 *Phys. Rev.* A **58** 2684
[9] Dey B K 2000 *J. Phys. A: Math. Gen.* **33** 4643
[10] Shapiro M and Brumer P 2003 *Principles of the Quantum Control of Molecular Processes* (New York: Wiley)
[11] Schirmer S G, Girardeau M D and Leahy J V 2000 *Phys. Rev.* A **61** 012101
[12] Fu H, Schirmer S G and Solomon A I 2001 *J. Phys. A: Math. Gen.* **34** 1679
[13] Peirce A P, Dahleh M A and Rabitz H 1988 *Phys. Rev.* A **37** 4950
[14] Shi S and Rabitz H 1989 *Chem. Phys.* **139** 185
[15] Ohtsuki Y, Zhu W and Rabitz H 1999 *J. Chem. Phys.* **110** 9825
[16] Yan Y, Gillilan R, Whitnell R, Wilson K and Mukamel S 1993 *J. Phys. Chem.* **97** 2320
[17] Ohtsuki Y, Nakagami K, Fujimura Y, Zhu W and Rabitz H 2001 *J. Chem. Phys.* **114** 8867
[18] Umeda H and Fujimura Y 2000 *J. Chem. Phys.* **113** 3510
[19] Baer R and Kosloff R 1997 *J. Chem. Phys.* **106** 8862
[20] Koch C P, Kluner T and Kosloff R 2002 *J. Chem. Phys.* **116** 7983
[21] Seke J 1990 *J. Phys. A: Math. Gen.* **23** L61
[22] Uchiyama C and Shibata F 1999 *Phys. Rev.* E **60** 2636
[23] Breuer H P, Kappler B and Petruccione F 2001 *Ann. Phys.* **291** 36
[24] Seke J, Soldatov A V and Bogolubov N N Jr 1997 *Mod. Phys. Lett.* B **11** 245
[25] Uchiyama C and Shibata F 1996 *J. Phys. Soc. Japan* **65** 887